

# The role of Joule heating in the formation of nanogaps by electromigration

M.L. Trouwborst,<sup>a</sup> S.J. van der Molen,<sup>b</sup> and B.J. van Wees  
*Physics of Nanodevices, Materials Science Centre, Rijksuniversiteit Groningen,  
Nijenborgh 4, 9747 AG Groningen, The Netherlands*  
(Dated: October 29, 2018)

We investigate the formation of nanogaps in gold wires due to electromigration. We show that the breaking process will not start until a local temperature of typically 400 K is reached by Joule heating. This value is rather independent of the temperature of the sample environment (4.2-295 K). Furthermore, we demonstrate that the breaking dynamics can be controlled by minimizing the total series resistance of the system. In this way, the local temperature rise just before break down is limited and melting effects are prevented. Hence, electrodes with gaps  $< 2$  nm are easily made, without the need of active feedback. For optimized samples, we observe quantized conductance steps prior the gap formation.

PACS numbers:

## I. INTRODUCTION

For single molecular electronics, electrodes are needed with a separation of typically one nanometer. In recent years, some creative methods have been developed to fabricate such devices. Some with tunable electrode distance, like scanning probe methods [1, 2] and mechanically controllable break junctions,[3, 4, 5] and others with a fixed distance, like electromigration-induced tunnel devices.[6, 7, 8] The latter have the advantage that they can easily be extended with a third (gate) electrode. Also, compared to other procedures, electromigration-induced nanogaps are easy to prepare, making this method one of the most promising techniques.

Electromigration-induced nanogaps are produced by applying large current densities to gold wires. At high current densities  $j$  (typically  $10^8 A/cm^2$ ), momentum transfer from the electrons to the gold atoms leads to drift of the atoms, in the direction of the electron flow. This mass flux can lead to the growth of voids in the wire, finally leading to the formation of gaps.[9] These gaps can have widths as small as a single nanometer, which makes them suitable for single molecular electronics.[10, 11] However, to obtain gaps smaller than 2 nm, it is crucial that the process is indeed dominated by electromigration. Joule heating, resulting in melting and surface tension effects, can be the cause of much bigger gaps and gold island formation.[12, 13, 14]

It is a challenging problem to prevent excessive heating. The reason for this is that a high current density is only one of the requirements for nanogap formation. An additional condition is that the atomic mobility is high enough for substantial mass flux to occur. Since the mobility shows activated behavior, the local temperature plays a key role in electromigration. If the temperature of

the sample environment is low (e.g., 77 K), Joule heating has to be substantial to induce the required local temperature. Below, we show, using a simple model and local temperature measurements, that gap formation typically takes place at a local temperature  $T_{start} \sim 400$  K. This value is rather independent of the temperature of the sample environment (4.2 K, 77 K, or 295 K).

Unfortunately, the local temperature does not stay constant once the breaking process has started. While the slit is being formed, the current density and, hence, the local Joule heating increases. As a consequence, the local temperature diverges just before break down. In fact, temperatures can be reached up to the melting point of gold, leading to ill-defined junctions. This problem can be solved by using an active feedback system, where the speed of the electromigration process is kept constant.[12, 13, 14, 15, 16] In this way, the temperature is limited, giving better control on the final gap size. In this article, we discuss a simple model to describe the local temperature rise just before break down. We test this model by doing local temperature measurements during the electromigration process. We show that excessive heating can be prevented, by limiting the series resistance of the system. This makes a feedback system unnecessary. By optimizing our sample design, we have increased the number of junctions with gaps  $< 2$  nm from 15 to  $> 90$  percent. Furthermore, constrictions of only one or a few atoms can easily be achieved, leading to conductance steps of typically  $2e^2/h$ .

## II. THEORY: ELECTROMIGRATION IN METALS

Electromigration is commonly described as a mass flux under the influence of a high current density. However, a full description of the electromigration problem is not trivial. To give some insight, we refer to thermodynamics of irreversible processes. This theory considers *all* fluxes and forces involved.[17] In our case, there are three types of fluxes to be dealt with: the electron particle flux ( $\mathbf{J}_e$ ),

<sup>a</sup>Electronic address: M.L.Trouwborst@rug.nl

<sup>b</sup>Present address: Nanocenter Basel, Institute of Physics, Klingelbergstrasse 82, CH-4056, Basel, Switzerland

the flux of metal atoms ( $\mathbf{J}_m$ ), and the energy flux ( $\mathbf{J}_u$ ). These fluxes are induced by a set of three 'forces' (or potential gradients),  $\mathbf{X}_j$ . For the particle forces, we can write  $\mathbf{X}_j = -\nabla\mu_{ec}^j$ . Here,  $\mu_{ec} = \mu + Ze\varphi$  is the electrochemical potential, with  $\varphi$ ,  $\mu$  and  $Z$ , the electrostatic potential, the chemical potential and particle charge (-1 for electrons), respectively. The other 'force' is due to a temperature gradient:  $\mathbf{X}_u = \nabla(1/T)$ . From thermodynamics of irreversible processes we have following set of equations:

$$\mathbf{J}_m = -L_{m,m}\nabla\left(\frac{\mu_{ec}^m}{T}\right) - L_{m,e}\nabla\left(\frac{\mu_{ec}^e}{T}\right) - L_{m,u}\left(\frac{\nabla T}{T^2}\right) \quad (1)$$

$$\mathbf{J}_e = -L_{e,m}\nabla\left(\frac{\mu_{ec}^m}{T}\right) - L_{e,e}\nabla\left(\frac{\mu_{ec}^e}{T}\right) - L_{e,u}\left(\frac{\nabla T}{T^2}\right) \quad (2)$$

$$\mathbf{J}_u = -L_{u,m}\nabla\left(\frac{\mu_{ec}^m}{T}\right) - L_{u,e}\nabla\left(\frac{\mu_{ec}^e}{T}\right) - L_{u,u}\left(\frac{\nabla T}{T^2}\right) \quad (3)$$

where the phenomenological constants  $L_{ij}$  relate all fluxes to all forces, whilst obeying the Onsager relations,  $L_{ij} = L_{ji}$ . The coupled equations above provide a general description of the system. This description includes electromigration as well as thermo-electric effects and thermodiffusion. The latter refers to a mass flux due to temperature gradients (which can, in turn, be due to Joule heating). Unfortunately, to solve the set of equations for a three-dimensional geometry is a formidable task. With a few assumptions, however, a simplified relation for the mass flux can be obtained. First, for materials with a high conductivity, we can ignore  $\nabla\mu^e$ . Second, we choose to neglect thermodiffusion. In the experimental part of this article, this assumption will be justified. Finally, we note that in practice all charge current is due to electron flux, so that  $-\nabla\varphi = \rho j$  (with  $\rho$  the electrical resistivity). Hence, we obtain:

$$\mathbf{J}_m = -L_{m,m}^*(\nabla\mu^m - Z^*e\rho j) \quad (4)$$

where we defined  $L_{i,j}^* = L_{i,j}/T$ . Furthermore, we introduced an effective charge  $Z^*$ :

$$Z^* = Z - \frac{L_{m,e}^*}{L_{m,m}^*} \quad (5)$$

In words, the atoms behave as if they had a charge  $Z^*$ . [17, 18, 19] This effective charge is due to momentum transfer from electrons to atoms. Generally,  $\frac{L_{m,e}}{L_{m,m}} \gg Z$ , so the net force acting on the gold atoms will be in the direction of the electron flow.

### III. EXPERIMENTAL SETUP

Two kinds of samples are fabricated on top of a 500 nm thick  $\text{SiO}_2$  layer on Si. For the first, called 'terrace samples', we use shadow evaporation and a resist bridge to obtain different thicknesses for the leads and the constriction (see Fig. 1a). In the constriction, 15 nm Au is evaporated, while for the leads 150 nm Au on top of 2 nm Cr is used. To decrease the constriction length, an extra 50 nm Au is evaporated. This way, a constriction of about  $250 \times 100$  nm (length  $\times$  width) is obtained. Due to thick gold leads, the total resistance is only 30  $\Omega$  (including the wires of the measurement setup). For the second kind of samples, called 'bow tie samples', we define a constriction in the shape of a bow tie with a minimum width of 20 to 60 nm. In this case, the thickness of the gold in the leads and the constriction is the same, namely 17 nm. Furthermore, a 3 nm adhesion layer is used for most of the gold structure. By evaporating this layer at an angle, we make sure that the Chromium does not reach the constriction. Therefore, the very center of the constriction contains gold only.

Electromigration is performed by applying a slowly increasing voltage (Keithley 230) to the wire, while monitoring the current (Keithley 6517A). Measurements were done at room temperature (in air) and at both 77 and 4.2 K (in cryogenic vacuum). After break down, tunnel currents were determined. In our setup, zero-bias tunnel resistances up to  $10^{12} \Omega$  can be measured.

### IV. RESULTS AND DISCUSSION

#### A. Excessive heating during electromigration

A typical graph of an electromigration experiment is shown in Figure 1b. Here, breaking is performed for a 'terrace sample' (Fig. 1a) by slowly increasing the voltage by 2 mV/s, at 77 K. The initial total resistance (including wiring) is 36  $\Omega$ . At about 0.38 V, the current density has reached a value that causes substantial mass flux, starting the formation of a slit. At 0.4 V, the wire finally breaks down. Subsequently, a small tunnel current can be observed, indicating that the gap size is around 1 nm.

A very different result is obtained for the experiment in Fig. 2. For this measurement, performed on a 'bow tie' sample, we added an extra series resistance. The total initial resistance equals 1780  $\Omega$ . Although the graph in Fig. 2a) looks similar to the one in Fig. 1b), there are some obvious differences. First, the breaking process is much more abrupt (see insets). Second, the voltage at break down is much higher (11 V vs. 0.4 V). The most dramatic difference is, however, that no tunnel current could be detected after break down. To investigate the gap in more detail, we used atomic force microscopy (AFM). In Figure 2b an AFM picture is shown of the 'bow tie' sample after the breaking process. The final gap size is approximately 100 nm, and the elec-

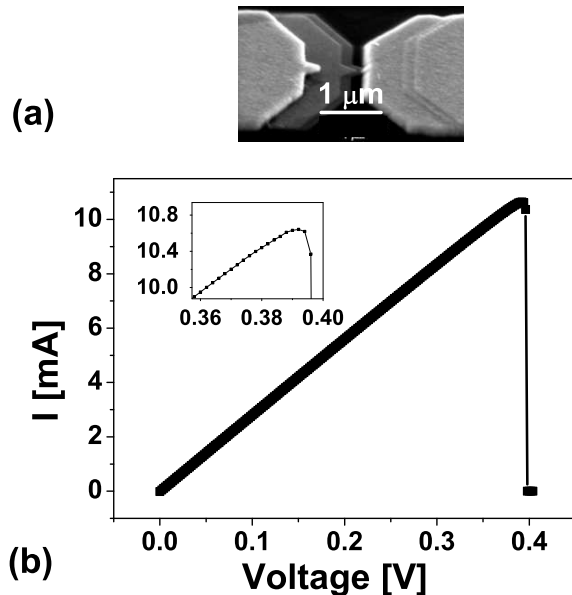


FIG. 1: a) Scanning electron micrograph of an electromigration sample, 'terrace' type, made with electron beam lithography. The thickness of the gold layer is 15 nm (middle), 50 nm, and 150 nm (leads). The constriction in the middle is about 100 nm in width. b) Representative breaking curve. The voltage is increased by 2 mV/s, while the current is observed. At 0.38 V, the electromigration process starts, leading to a decrease in current. At 0.4 V, after break down, a tunnel current can be measured of about 500 nA. Inset: magnification of region just before break down. Due to temperature increase and electromigration,  $dI/dV$  decreases slowly, until final break down occurs. Measurement at 77 Kelvin, the initial total resistance is 36  $\Omega$ .

trodes have clearly rounded off. Most likely this is due to local melting. Furthermore, there is a set of gold islands in between the electrodes. We note that the presence of such nanoparticles may lead to Coulomb blockade effects.[13, 14, 20, 21] From Figure 2b we conclude that the break down process has taken place in an uncontrolled manner, leading to high local temperatures (and fields). We shall show below, that the breaking dynamics is strongly correlated with the resistance in series with the constriction,  $R_s$ . We note that this resistance constitutes the main difference between the experiments in Figures 1 and 2. Minimizing  $R_s$ , results in a much better control of the final gap size, making a feedback system unnecessary.

To demonstrate the significance of  $R_s$ , we use a simple model for the constriction (a schematic drawing is shown in Fig. 3). We consider a slit of length  $l$ . Its width  $w(t)$  and height  $h(t)$  are decreasing functions of time, due to gap formation. The total resistance,  $R_{tot}$ , is the sum of the constriction resistance,  $R_c(t) = \frac{\rho l}{h(t)w(t)}$ , and a series resistance  $R_s$ . In a virtual experiment, we ramp up the voltage until electromigration begins at a bias  $V = V_c$

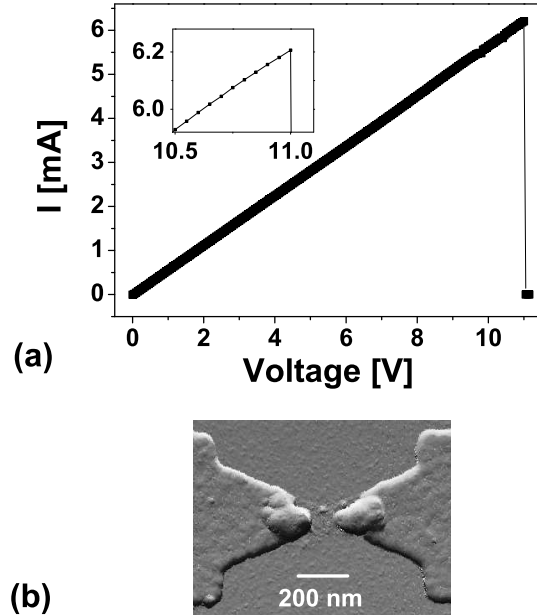


FIG. 2: a)  $I(V)$  measurement during an electromigration experiment ('bow tie' sample). The total resistance before electromigration is 1780  $\Omega$ . At 11 V, the sample breaks down abruptly. No tunnel current could be observed afterwards. Inset: Magnification of region just before breaking. Measurement at 295 K. b) AFM picture of the sample after breaking. As can be seen, the breaking mechanism for this sample was melting instead of electromigration. In between the electrodes, gold islands can be observed.

(at  $t \equiv 0$ ). A more accurate way of saying that 'electromigration begins' is to say that the flux of gold atoms,  $J_m$ , reaches a certain critical value  $J_m^c$ . [22] For this to happen, both the current density  $j$  and the mobility (related to  $L_{m,m}^*$  in eq. (4)) need to be substantial. The mobility is strongly affected by the local temperature, which increases due to Joule heating via  $p = \rho j^2$ . Consequently, electromigration does not start, until a certain combination of current density  $j_c$  and local temperature  $T_{start}$  is reached. The latter is directly related to the local dissipation  $p_c = \rho j_c^2$  (below, we discuss this in more detail). [23] The voltage  $V_c$  and local dissipation  $p_c$  are related by  $p_c = \frac{V_c^2}{\rho l^2} / (1 + \frac{R_s}{R_c(0)})^2$ . Next, we consider the breaking process for  $t > 0$ , keeping the voltage constant at  $V = V_c$ . Due to electromigration a slit is formed in the constriction, leading to an increasing constriction resistance  $R_c(t)$ . Consequently, the local dissipation also increases, according to (in the diffusive regime):

$$p(t) = p_c \left( \frac{1 + \frac{R_s}{R_c(0)}}{1 + \frac{R_s}{R_c(t)}} \right)^2 \quad (6)$$

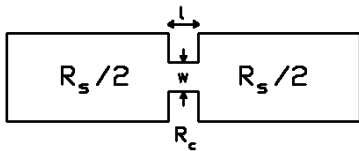


FIG. 3: Schematic presentation of an electromigration sample. The total resistance  $R$  consists of the constriction resistance  $R_c$  and series resistance  $R_s$ . Due to electromigration, the constriction will shrink in time, leading to a reduction of the width  $w$  and height  $h$  and an increase of  $R_c$ .

Let us first consider the limit with a small series resistance,  $\frac{R_s}{R_c(0)} \ll 1$ . In this case, the dissipated power is always equal to  $p_c$ , independent of the width of the constriction. Hence, the local temperature stays close to  $T_{start}$  and the gap grows slowly in time. In the other limit,  $\frac{R_s}{R_c(0)} \gg 1$ , the situation is different. At the start of the process ( $t=0$ ), the local power equals  $p_c$ . However, the dissipated power increases rapidly during the breaking process, especially when  $R_c(t) \gg R_c(0)$ . In this limit,  $p \gg p_c$ . Consequently, uncontrollable heating takes place. This can finally lead to melting of the electrodes.[24] We note that equation (6) only holds in the diffusive regime, where the mean free path of the electrons is much smaller than the dimensions of the contact. Interestingly, as the electromigration process continues, the size of the constriction decreases. Provided that heating is limited, one expects a cross-over from the diffusive to the ballistic transport regime. We will return to this phenomenon in section C.

To have a better control of the final gap size, one has to limit the series resistance within the set-up as well as within the sample itself. For the latter we developed the 'terrace' samples that connect big leads to the constriction (see Fig. 1a). As compared to the 'bow tie' samples (see Fig. 2b), this geometry has three advantages. The most important one is to limit the dissipated power during electromigration, by the reduction of  $R_s$ . Another advantage is that the voltage needed to break the samples is limited. This is important, since, after break down all the voltage drop will be across the gap. This leads to a high electric field. It is well known that electric fields exceeding 2 V/nm, can cause a reorganization of the electrodes. Depending on the shape of the electrodes, this reorganization can result in a larger gap size.[25, 26] A third advantage of thick leads, is their use as heat sinks. In this way, the heat can easily flow away from the constriction. By the evaporation of 150 nm Au for the leads, we have a total resistance of typically 30  $\Omega$  (including the wiring of the measurement setup).

To show the effect of a series resistance experimentally, a variable resistance is inserted in series with the sample. This way, we can check the final gap size as a function of  $R_s$ . The result is shown in Fig. 4. We have investigated 142 samples, of both types. The wires were broken by

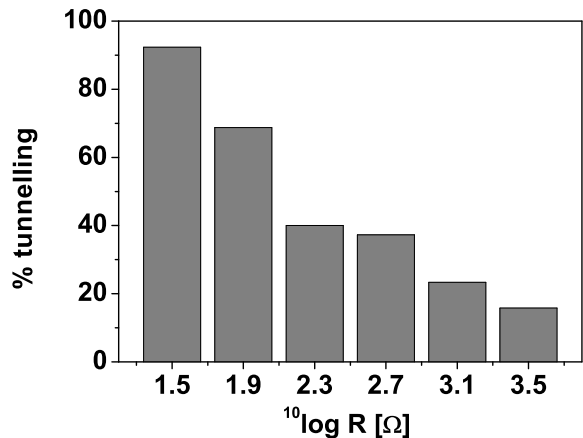


FIG. 4: Percentage of samples with a zero-bias tunnel resistance  $< 10^{12}$  Ohm after electromigration, as a function of the initial series resistance. High initial series resistances lead to excessive heating, causing large gaps. The number of samples showing a tunnel current can be increased from 15 up to  $> 90$  percent by limiting the series resistance. In total, 142 samples were measured. The number of samples per bar is 13/16/5/59/30/19.

slowly increasing the voltage until a gap occurs. Afterwards, the tunnel resistance at zero bias was measured, in order to make an estimation of the gap size. Zero bias resistances larger than  $10^{12}$   $\Omega$  could not be measured, and are counted as "no tunnelling". As can be seen from Fig. 4, there is a strong relation between the gap size and the total initial resistance. Considering samples with large series resistances, from 2 – 8  $k\Omega$ , only 15 percent have nanogaps with a measurable tunnel current. Samples with low series resistances, however, give smaller gaps. Decreasing the value for the series resistance to about 30  $\Omega$ , gives nanogaps with a measurable tunnel current in more than 90 percent of the cases. From the tunnel current, an estimation can be made of the size of the gaps. These are in the range of 0 to 2 nm.

## B. Local temperature during electromigration

For the model discussed above, we assumed that gap formation does not start until a certain critical temperature  $T_{start}$  is reached. To test if this is indeed the case, we performed measurements at 4.2, 77 and 295 Kelvin. We found no clear differences in final gap size. We did observe, however, that a higher critical power  $p_c$  is needed, when samples are broken at lower temperatures. This suggests that the local temperature at which electromigration is triggered, is more or less independent of the surrounding temperature. This is as expected, since the mobility of gold atoms is strongly dependent on the temperature (we will discuss this in more detail below).

In order to find the local temperature during elec-

tromigration,  $T_{em}$ , we fabricated four terminal devices. Knowledge of  $T_{em}$  is important, since, for molecular electronics, molecules are often put on the sample prior the breaking process. High temperatures could damage the molecules, right where the nanogap will be formed.

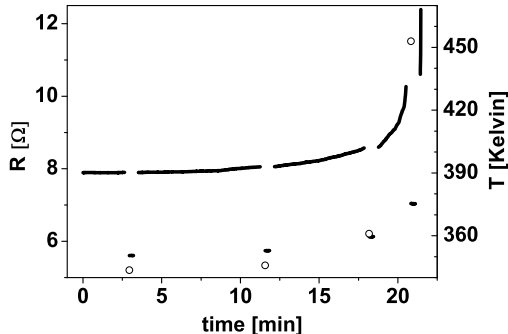


FIG. 5: Four-terminal resistance during electromigration. The voltage is set for an initial electromigration speed of  $100 \mu\Omega/s$ , and kept constant afterwards. Due to electromigration, grain coalescence and heating, the resistance increases. Every couple of minutes, the resistance is measured at low voltage, and then  $V$  is set back to the initial value. From the change in resistance between low and high voltage, the average local temperature can be obtained (circles). The temperature of the environment is 77 K, while the temperature at which electromigration is initiated is 345 K. Just before break down, the temperature increases. The last temperature measured before break down is 450 K. The applied voltage is 0.72 V. The initial two-terminal resistance is  $41 \Omega$ , the four-terminal resistance is  $5.8 \Omega$  (at 77 K). The initial current density is  $4 \times 10^8 A/cm^2$ .

To determine the local temperature, the samples were first cooled down to obtain the relation between temperature and (local) resistance ( $4.2 \text{ K} < T < 295 \text{ K}$ ). [27, 28, 29] The electromigration experiment is subsequently performed as follows. First, the voltage is increased till electromigration starts (defined as  $dR/dt = 100 \mu\Omega/s$ ), and kept constant afterwards. An example is shown in Fig. 5. From here on, different processes will influence the local resistance. The most important ones are electromigration, heating and the coalescence of grains. To make an estimation of  $T_{em}$ , it is crucial to deduce only the resistance change due to heating. This was done by interrupting the measurement every couple of minutes, and determining the resistance at low voltage. [28] Finally, the average local temperature  $T_{em}$  is estimated from the resistance difference at low and high voltage and the (extrapolated) relation between temperature and resistance.

For the trace in Fig. 5, the initial four-terminal resistance was  $5.8 \Omega$  (at 77 Kelvin). Setting the voltage to start the breaking process, increases the resistance drastically to about  $8 \Omega$  (due to heating). Subsequently, the resistance increases in time, and accelerates just before breaking. Furthermore, the local temperature increases,

TABLE I: Local temperature at which electromigration starts,  $T_{start}$ , for 5 different samples. Interestingly,  $T_{start}$  appears rather independent of the temperature of the sample surroundings,  $T_0$ . For data set C and E, the temperature is also measured just before break-down,  $T_{final}$ . This temperature depends strongly on to what extent the process is controlled. Data set C is taken from Fig. [5].

Data set	$T_0[K]$	$T_{start}[K]$	$T_{final}[K]$
A	4.2	$430 \pm 40$	–
B	4.2	$440 \pm 40$	–
C	77	$345 \pm 10$	$455 \pm 10$
D	295	$380 \pm 40$	–
E	295	$420 \pm 10$	$460 \pm 10$

as predicted by eq. (6). We note that there is always some series resistance, so that heating cannot be taken away completely. However, when high series resistances are used, the temperature does not only reach higher values, it also diverges much faster. This is clearly shown in the insets of Figures 1b and 2a. In Fig. 1b, a slow increase in differential resistance is observed. In contrast, for Fig. 2b, gap formation goes all at once, and the breaking process cannot be resolved.

In Fig. 5, the local temperature increases from 77 K to 345 K, when the voltage is set to start the breaking process. The temperature determined just before break down,  $T_{final}$ , is about 450 Kelvin. In Table [I], four other data sets are shown, at different environment temperatures. The temperatures at which electromigration is triggered are close together, whereas the variation in the temperature of the environment is about 290 Kelvin. This is a strong indication that gap formation is indeed due to electromigration (at a critical temperature) and not due to thermodiffusion via a temperature gradient. [29]

To understand why  $T_{start}$  is rather independent of the temperature of the sample environment,  $T_0$ , we introduce a simple model. To fit its parameters, we use the data taken at 77 K (Fig. 5). We rewrite eq. (4), by noting that  $\nabla\mu^m = \Omega d\sigma/dx$  is the driving force due to stress  $\sigma$ : [19, 30]

$$\mathbf{J}_m = -L_{m,m}^*(\Omega\Delta\sigma/L - Z^*e\rho j) \quad (7)$$

Here  $\Delta\sigma$  is the stress built up over the length  $L$ . As long as  $\Delta\sigma < \Delta\sigma_{max}$ , the electromigration force is balanced by the stress gradient and the atom flux  $J_m$  is zero. [19, 30] This defines a critical current density  $j_{min} = \frac{\Omega\Delta\sigma_{max}}{Z^*e\rho L}$ , which is independent of temperature, since  $Z^*\rho$  is temperature independent. [31, 32] Using the Einstein relation  $D = L_{m,m}^*d\mu/dc$ , where  $D$  and  $c$  are the diffusion constant and concentration respectively, we can write down the temperature dependence of the atom flux. For the chemical potential we have  $\mu = kT \ln c$ , [19] and for the diffusion constant  $D = D_0 e^{-E_a/kT}$  so that we can write for the phenomenological coefficient:  $L_{m,m}^* =$

$\frac{D_0}{kT} ce^{-E_a/kT}$ . Here,  $E_a$  is the activation energy of gold diffusion on the surface, which is 0.12 eV.[33] This leads to the following approximation for the atom flux due to the current density:

$$\mathbf{J}_m = \frac{\alpha}{T}(j - j_{min})e^{-E_a/kT} \quad (8)$$

where  $\alpha \equiv cD_0Z^*e\rho/k < 0$ . For our measurements we use temperatures in between liquid Helium and Room temperature and the applied voltage over the constriction is typically 20 mV or higher. In this range, the inelastic scattering length of the electrons does not exceed the contact size. Therefore, the effective temperature in the contact can be described by  $T = T_0 + \beta j^2$ , where  $\beta$  is a fit parameter.[34] We determine  $\beta$  from the first temperature point in Fig. 5:  $T_{start} = 345$  K at  $j = 4 \times 10^8$  A/cm<sup>2</sup>. Furthermore, we estimate that  $j_{min}$  equals  $j_{min} \approx 1 \times 10^8$  A/cm<sup>2</sup>. [19]

Equation [8] implies a strong relation between temperature and mass flux, especially due to the activated behavior. Gap formation starts as soon as the mass flux is large enough, i.e., when  $J_m$  reaches a certain value  $J_m^c$ . We define this quantity, in arbitrary units, as  $J_m^c \equiv 1$ . Going back to Fig. 5 with  $T_0 = 77$  K, we infer that for  $j = 4 \times 10^8$  A/cm<sup>2</sup>, we have  $J_m = J_m^c = 1$ . From this, we deduce the other parameter  $\alpha$ . Knowing both  $\alpha$  and  $\beta$ , we can plot  $J_m$  as a function of current density  $j$  for all three experimental temperatures  $T_0$ . This is shown in Fig. 6. For each  $T_0$ , we calculate the current density and temperature at which electromigration sets in,  $T_{start}$ , demanding  $J_m = 1$ . (For  $T_0 = 77$  K, this is by definition at  $j = 4 \times 10^8$  A/cm<sup>2</sup> with  $T = 345$  K). For  $T_0 = 4.2$  K and  $T_0 = 295$  K we find that  $T_{start}$  equals 330 and 420 K, respectively. Hence, increasing the temperature of the environment by 290 K, increases  $T_{start}$  by only 90 K. Related to this is the fact that the critical current density increases with decreasing  $T_0$ . Although basic, the model is in rather good agreement with the values of Table [I].

Do previously applied molecules get damaged at these temperatures? As we have shown above, the local temperature just before break down depends on the exact sample design. Also, the maximum temperature molecules can stand, strongly depends on the molecule. At 460 Kelvin, which is  $T_{final}$  in Table [I], most molecules used in molecular electronics, do not get damaged. However, care should clearly be taken. The electromigration process should be controlled either by optimizing the sample design, or by using active feedback. If not, the local temperature increases dramatically as the wire gets thinner and may reach values up to the melting point of gold.

### C. Quantized conductance

As we have shown, decreasing the series resistance gives a better control of the final gap size. Another interesting consequence of controlled electromigration, is

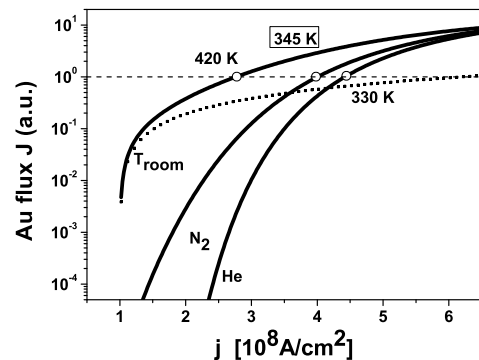


FIG. 6: Mass flux  $J_m$  (arbitrary units) versus current density  $j$ , for various surrounding temperatures  $T_0$  (see eq. (8)). From Fig. [5], we know that electromigration starts (i.e., that  $J_m = 1$ ) when  $j = 4 \times 10^8$  A/cm<sup>2</sup> with a local temperature  $T_{start} = 345$  K (rectangle). We use this to obtain the parameters  $\alpha$  and  $\beta$  in eq. (8). With these,  $J_m$  versus  $j$ , can also be plotted for  $T_0 = 4.2$  K and  $T_0 = 295$  K, respectively. Taking Joule heating into account (solid lines), the temperature at which electromigration starts is 330 K for  $T_0 = 4.2$  K and 420 K for  $T_0 = 295$  K, respectively. Note that when Joule heating is neglected, electromigration can only set in at room temperature (dotted line). For 4.2 and 77 K, the critical mass flux ( $J_m = 1$ ) cannot be reached for reasonable  $j$ .

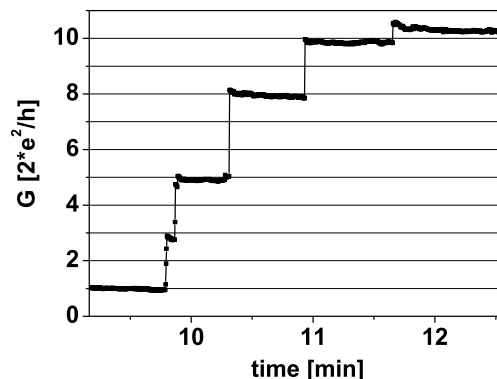


FIG. 7: Quantized conductance during the electromigration procedure at constant voltage. The voltage is set for an initial electromigration speed of  $100 \mu\Omega/s$ , starting the breaking process. The resistance increases due to electromigration until, after 9 minutes, a conductance of  $1 \times 2e^2/h$  is observed. After another minute, the configuration starts to reorganize, leading to a stepwise increase in conductance. Measurement at room temperature with  $V = 0.73$  V and  $P = 1 \times 10^{-6}$  mbar.

the possibility to observe the transition between the diffusive and the ballistic regime.[12] If slit formation is a well-defined process, at some point the constriction gets smaller than the inelastic scattering length. In this case, conduction becomes ballistic. This is indeed what we observe in a number of cases. During the breaking process,

the sample conductance does not go smoothly to the tunneling regime, but locks in at plateaus equal to integer values of the conductance quantum  $2e^2/h$ . [35, 36] An example is shown in Fig. 7. Here, we start with a resistance of about  $45 \Omega$ , increase the voltage until we see a change in conductance and, from there on, keep the voltage constant. Slowly, the conductance goes down, to finally stop at  $1 \times 2e^2/h$ . At this point, the electromigration process stops automatically, due to the almost perfect transmission of the gold atoms. The corresponding current density is about  $57 \mu A/\text{atom}$ . This is close to the maximum value described elsewhere, [37] and is much larger than the maximum current density in the diffusive regime. Nevertheless, the electrodes reorganize due to atomic diffusion. Slowly, the contact evolves from a single atom contact to a contact with 3, 5, 8 and 10 gold atoms. [38] At much higher voltages, it is still possible to break the constriction and obtain a tunnel resistance. We note that we have only observed quantized conductance in samples with minimized  $R_s$ . If the power is unlimited, the high temperature prohibits the formation of a single atom contact.

## V. CONCLUSIONS

To conclude, we have investigated the role of dissipation during the formation of nanogaps due to electromigration. We find the following. First, some Joule heating is needed for gap formation to begin. The process does not start until a local temperature of typically 400 K is reached. This value is rather independent of the temperature of the surroundings. We relate this phenomenon to the activated behavior of the atomic mobility, which plays a crucial role in this diffusion process. Second, although Joule heating is important to start electromigration, it can also lead to unwanted effects. If no measures are taken, the temperature in the constriction can increase up to the melting point of gold, during slit formation. This leads to large gaps, possibly containing small gold islands. By minimizing the total series resistance of the system, we make sure the temperature keeps low during the electromigration process. In this way, we increased the number of samples with a gap  $< 2 \text{ nm}$  to  $> 90$  percent, without the use of active feedback. With the improved samples, gap formation is much slower. Hence, it is also possible to observe the transition from the diffusive to the ballistic regime. In a number of cases, contacts have been achieved that consist of only a single or a few atoms.

## Acknowledgments

We thank Gert ten Brink, Niko Tombros, Bernard Wolfs and Siemon Bakker for their assistance and advice. We thank Herre van der Zant and Hubert Heersche for useful discussions. This work was financed by the Ned-

erlandse Organisatie voor Wetenschappelijk Onderzoek, NWO, via a Pionier grant.

- 
- [1] B. Xu and N.J. Tao, *Science* **301**, 1221, (2003)
- [2] Bumm, L.A., Arnold, J.J., Cygan, M.T., Dunbar, T.D., Burgin, T.P., Jones II, L., Allara, D.L., Tour, J.M. and Weiss, P.S., *Science* 1996, 271, 1705-1707
- [3] R.H.M. Smit, Y. Noat, C. Untiedt, N. D. Lang, M.C. van Hemert and J.M. van Ruitenbeek, *Nature* 419 (2002) 906
- [4] D. Dulic, S.J. van der Molen, T. Kudernac, H.T. Jonkman, J.J.D. de Jong, T.N. Bowden, J. van Esch, B.L. Feringa, B.J. van Wees, *Phys. Rev. Lett.* **91**, 207402, (2003)
- [5] J. Reichert, R. Ochs, D. Beckmann, H.B. Weber, M. Mayor and H.V. Lohneysen, *Phys. Rev. Lett* **88**, 176804, (2002)
- [6] H. Park, J. Park, A. K. L. Lim, E. H. Anderson, A. P. Alivisatos, and P. L. McEuen, *Nature (London)*, **407**, 57 (2000)
- [7] W. Liang, M. P. Shores, M. Bockrath, J. R. Long, and H. Park, *Nature (London)*, **417**, 725 (2002)
- [8] J. Park, A. N. Pasupathy, J. I. Goldsmith, C. Chang, Y. Yaish, J. R. Petta, M. Rinkoski, J. P. Sethna, H. D. Abruna, P. L. McEuen, et al., *Nature (London)*, **417**, 722 (2002)
- [9] M. Mahadevan and R.M. Bradley, *Phys. Rev. B.* **59**, 11037 (1999)
- [10] H. Park, A. K. L. Lim, J. Park, A. P. Alivisatos, and P. L. McEuen, *Appl. Phys. Lett.* **75**, 301 (1999)
- [11] K. I. Bolotin, F. Kuemmeth, A. N. Pasupathy, and D. C. Ralph, *Appl. Phys. Lett.* **84**, 3154 (2004)
- [12] D.R. Strachan, D.E. Smith, D.E. Johnston, T.-H. Park, M.J. Therien, D.A. Bonnel and A.T. Johnson, *Appl. Phys Lett.* **86**, 43109 (2005)
- [13] H.B. Heersche, Z. de Groot, J.A. Folk, L.P. Kouwenhoven and H.S.J. van der Zant, A.A. Houck, J. Labaziewicz and I.L. Chuang, *Phys. Rev. Lett.* **96**, 017205, (2006)
- [14] A.A. Houck, J. Labaziewicz, E.L. Chan, J.A. Folk and I.L. Chuang, *Nano Letters* **5**,1685, 9 (2005)
- [15] G. Esen and M. S. Fuhrer , *Appl. Phys Lett.* **87**, 263101 (2005)
- [16] H.S.J. van der Zant *et al.*, *Faraday Discuss.*, **131**, 347 (2006)
- [17] S.R. de Groot, *Thermodynamics of irreversible processes*, North-Holland Publishing company, Amsterdam, (1963)
- [18] S.J. van der Molen, M.S. Welling and R. Griessen, *Phys. Rev. Lett.* **85**, 3882 (2000)
- [19] King-Ning Tu, J.W. Mayer, L.C. Feldman, *Electronic thin film science for electrical engineers and materials scientists*, Macmillan, New York, (1992)
- [20] J.I. Gonzalez, Tai-Hee Lee, M.D. Barnes, Y. Antoku and R.M. Dickson, *Phys. Rev Lett.* **93**, 147402(2004)
- [21] R. Sordan, K. Balasubradamanian, M. Burghard and K. Kern, *Appl. Phys Lett.* **87**, 013106 (2005)
- [22] For this manuscript we define the starting point of gap formation, when the increase in resistance reaches a speed of  $100 \mu\Omega/s$ . We note that for other values, the starting temperature  $T_{start}$  will also change.
- [23] Since we use a 1-dimensional model, the length of our constriction does not change with time.
- [24] A comparison can also be made with a current source (Norton equivalent circuit) and a voltage source (Thevenin circuit). Gold wires with high series resistances are broken as if connected to an ideal current source. As the width of the wire decreases, the current



density increases. Constrictions with negligible series resistances are broken as if connected to an ideal voltage source. As the width decreases, the current density stays approximately constant.

- [25] J. Mendez, J. Gomez-Horrero, J.I. Pascual, J.J. Seanz, J.M. Soler and A.M. Baro, *J. Vac Sci. Technol. B* **14**, 1145 (1996)
- [26] D. Huang, F. Yamaguchi, Y. Yamamoto, *Jap. Journal Appl. Phys.* **37**, 3824 (1998)
- [27] M. F. Lambert, M. F. Goffman, J. P. Bourgoin, and P. Hesto, *Nanotechnology* **14**, 772 (2003).
- [28] B. Stahlmecke and G. Dumpich, *Defect and Diffusion Forum Vols.* **237-240** 1163 (2005)
- [29] C. Durkan, M.E. Welland, *Ultramicroscopy* **82**, 125, (2000)
- [30] I.A. Blech, *J. Appl. Phys.* **47**, 1203 (1976)
- [31] R.S. Sorbello, *Solid State Phys.* **51**, 159-231 (1998)
- [32] A.H. Verbruggen, *IBM J. Res. Develop.* **32**, 93 (1988)
- [33] N.T. Wilson, *The structure and dynamics noble metal clusters*. PhD thesis, University of Birmingham, (Sept. 2000)
- [34] In our measurement range, the applied bias voltage is close to the Debye energy, leading to strong electron-phonon scattering. The inelastic scattering length does not exceed the contact size and the temperature in the contact can be described by the given relation. However, When temperatures around or below 1 Kelvin are considered, and the maximum voltage is in the mV range, electron-electron scattering is the dominant relaxation mechanism. The relation for the temperature becomes  $T = \sqrt{T_0^2 + \beta j^2}$ . For the measurement at Helium temperature, however, this will give only a minor change in the final maximum temperature (343 K instead of 330 K).
- [35] B.J. van Wees *et al.*, *Phys. Rev. Lett.* **60**, 848 (1988)
- [36] C.J. Muller, J.M. van Ruitenbeek and L.J. de Jongh, *Phys. Rev. Lett.* **69**, 140 (1992)
- [37] J. Mizobata, A. Fujii, S. Kurokawa, A. Sakai, *Phys. Rev. B* **68**, 155428 (2003)
- [38] Since it is not possible to vary the conductance back and forth, as with the mechanically controllable break junctions, we have not performed statistics. However, since the values are exactly equal to the conductance quantum, there is a strong indication that the conductance steps are due to single gold atoms.